A new reptile from the lower Permian of Brazil (*Karutia fortunata* gen. et sp. nov.) and the interrelationships of Parareptilia

Juan Carlos Cisneros , Christian F. Kammerer , Kenneth D. Angielczyk , Jörg Fröbisch , Claudia Marsicano , Roger M. H. Smith & Martha Richter

View supplementary material

Published online: 12 Jan 2021.

Submit your article to this journal

Article views: 107

View related articles

View Crossmark data

A new reptile from the lower Permian of Brazil (*Karutia fortunata* gen. et sp. nov.) and the interrelationships of Parareptilia

Juan Carlos Cisneros[a]* (iD), Christian F. Kammerer[b] (iD), Kenneth D. Angielczyk[c], Jörg Fröbisch[b,d] (iD), Claudia Marsicano[e,f] (iD), Roger M. H. Smith[g,h] (iD) and Martha Richter[i] (iD)

[a]*Museu de Arqueologia e Paleontologia, Universidade Federal do Piauí, 64049-550 Teresina, Brazil;* [b]*Paleontology Unit, North Carolina Museum of Natural Sciences, Raleigh, NC 27601, USA;* [c]*Negaunee Integrative Research Center, Field Museum of Natural History, 1400 South Lake Shore Drive, Chicago, IL 60605, USA;* [d]*Institut für Biologie, Humboldt-Universität zu Berlin, Invalidenstr. 42, D – 10115 Berlin, Germany;* [e]*Departamento de Cs. Geologicas, FCEN, Universidad de Buenos Aires, C1428EHA Ciudad Autónoma de Buenos Aires, Argentina;* [f]*CONICET-UBA, Instituto de Estudios Andinos (IDEAN) Buenos Aires, Argentina;* [g]*Evolutionary Studies Institute, University of the Witwatersrand, Private Bag 3, 2050 Johannesburg, South Africa;* [h]*Iziko South African Museum, PO Box 61, Cape Town, South Africa;* [i]*Department of Earth Sciences, Natural History Museum, Cromwell Road, London SW7 5BD, UK*

A new parareptile from the Cisuralian Pedra de Fogo Formation of north-eastern Brazil is described. *Karutia fortunata* gen. et sp. nov. is the first Gondwanan member of Acleistorhinidae, a clade previously known only from North America but thought to be closely related to the Russian Lanthanosuchidae. A re-examination of parareptile phylogeny indicates that lanthanosuchids are not closely related to acleistorhinids. These results are more congruent both stratigraphically and biogeographically than the previous 'lanthanosuchoid' position for acleistorhinids, as they eliminate a 15 Ma ghost lineage within parareptiles, leaving Acleistorhinidae as an exclusively Pennsylvanian/Cisuralian clade from western Pangaea. *Karutia fortunata* contributes to our knowledge of the early Permian diversity of Parareptilia in Gondwana, a clade previously represented only by the mesosaurid inhabitants of the Irati-Whitehill epicontinental sea in the southern portion of the supercontinent. The new parareptile joins captorhinids in the amniote record of the Pedra de Fogo Formation, improving our picture of the inland tetrapod fauna of the southern hemisphere during the Cisuralian.

http://zoobank.org/urn:lsid:zoobank.org:pub:79D59764-4DA0-4C28-B4D3-C517BBF64D81

Keywords: Reptilia; Parareptilia; Acleistorhinidae; Gondwana; Cisuralian; Pedra de Fogo Formation; Parnaíba Basin

Introduction

Parareptilia is a reptile lineage that first appeared in the late Carboniferous (Modesto *et al.* 2015; Mann *et al.* 2019) and underwent major evolutionary radiations during both the Permian and Triassic periods (Tsuji & Müller 2009; Ruta *et al.* 2011; MacDougall *et al.* 2019a). This morphologically disparate group produced bauplans ranging from the small, facultatively bipedal bolosaurs to the fully aquatic mesosaurs and the large, armoured pareiasaurs, and repeatedly acquired dental adaptations for insectivory, low- and high-fibre herbivory, and durophagy (Reisz & Sues 2000; Reisz 2006; Cabreira & Cisneros 2009). The fossil record of parareptiles is extensive, with much of their history characterized by an exceptionally high-quality record as reflected by mean specimen completeness (Verrière *et al.* 2016).

The placement of parareptiles within Amniota has been the subject of recent debate (Laurin & Piñeiro 2017, 2018; MacDougall *et al.* 2018, 2019b; Ford & Benson 2020). Many parareptilian subclades are highly autapomorphic and the paucity of generalized taxa has complicated analyses of their relationships. Although frequently recovered as the sister group of all other parareptiles (e.g. Modesto 2006), Mesosauridae consists of highly specialized aquatic forms that provide little insight into the ancestral morphology of parareptiles. Greater potential for understanding the plesiomorphic condition in parareptiles comes from small, terrestrial and superficially 'lizard-like' Permo–Carboniferous taxa such as bolosaurs and acleistorhinids. Acleistorhinidae historically was a very poorly known group, originally represented only by *Acleistorhinus pteroticus* Daly, 1969 from the lower Permian of Oklahoma, USA, which was recognized as a basal parareptile in the 1990s (deBraga & Reisz 1996; Modesto 1999). Work in the last two decades has greatly expanded our knowledge of Acleistorhinidae, revealing a number of new taxa from North America. Most of these taxa are based on

*Corresponding author. Email: juan.cisneros@ufpi.edu.br

discoveries at the Richards Spur site in Oklahoma, a locality that has demonstrated that parareptilian diversity was comparable to that of Eureptilia during the Cisuralian (MacDougall *et al*. 2017). In addition to these Permian finds, the acleistorhinid *Carbonodraco lundi* from the middle Pennsylvanian of Ohio, USA, has recently been identified as the oldest known parareptile (Mann *et al*. 2019). Members of the Acleistorhinidae are characterized by cranial sculpturing, usually in the form of pits; size-related heterodonty (frequently with plicidentine on the enlarged teeth); and (ontogenetically and taxonomically) variable temporal openings (MacDougall & Reisz 2014; MacDougall *et al*. 2014; Haridy *et al*. 2016). All acleistorhinid species so far known have been found in North America and are represented mainly by cranial material.

The highly specialized mesosaurs, which inhabited the saline (and in parts anoxic) Irati/Whitehill inland sea in southern Gondwana (e.g. Piñeiro *et al.* 2012), have long been the only parareptiles (and amniotes in general) known from the lower Permian of the southern hemisphere. Recent research in the Pedra de Fogo Formation, near the city of Teresina within the Parnaíba Basin of north-eastern Brazil, has revealed a new lower Permian tetrapod fauna associated with an alkaline lacustrine/wetland system (Cisneros *et al.* 2015; Iannuzzi *et al.* 2018). This tetrapod assemblage is dominated by temnospondyls, with amniotes being represented by at least two captorhinid morphotypes, including the genus *Captorhinikos*, previously known only from the Cisuralian of North America (Cisneros *et al.* 2020). Collecting efforts in 2016 revealed a third amniote from this formation, represented by cranial and postcranial remains here identified as the first Gondwanan acleistorhinid parareptile.

Material and methods

The specimen (Fig. 1) was discovered in a small sandstone slab in a paving stone quarry in Nazária, Piauí. Most of the bony elements were disarticulated and broken yet still closely associated. The specimen was mechanically prepared using fine needles and a PaleoTools Micro Jack 1 pneumatic air scribe. Some bones were detached from the block and individually prepared on a bed of polyethylene glycol. Fibreglass filaments embedded in paraloid B-72 were attached to individual bones that, due to their fragility, required additional support.

A cladistic analysis was carried out using an expanded version of the character-taxon matrix of MacDougall *et al.* (2017). Two characters were deleted, one character was split into two new characters, three were modified and a total of 14 new characters were added (see Supplementary material). Eighty-four character state codings were

reassessed based, as much as possible, on first-hand examination of fossils and supported by the literature (see Table 1 for specimens and references). The recently recognized parareptile *Carbonodraco lundi* from the Pennsylvanian of the USA was added to the matrix, with its scoring based on the description of Mann *et al.* (2019). See the supporting information for the data matrix, new characters included in the analysis, and alterations to previous characters and scorings. The character-taxon matrix was compiled in Mesquite v. 3.2 (Maddison & Maddison 2018), and the phylogenetic analysis was performed using TNT v. 1.5 (Goloboff & Catalano 2016). A traditional (heuristic) search was carried out using tree bisection reconnection and saving 10 trees per replicate. All characters were unordered and unweighted, ambiguously supported branches were collapsed ('collapsing rule 1') and *Seymouria* served as the outgroup taxon. Symmetric resampling (Goloboff *et al.* 2003) support values were calculated from 5000 replicates.

Institutional abbreviations

BP, Evolutionary Studies Institute, University of the Witwatersrand, Johannesburg, South Africa; **FMNH,** Field Museum of Natural History, Chicago, USA; **MAP,** Museu de Arqueologia e Paleontologia, Universidade Federal do Piauí, Teresina, Brazil; **OMNH,** Sam Noble Oklahoma Museum of Natural History, Norman, USA; **PIN,** Borissiak Palaeontological Institute, Russian Academy of Sciences, Moscow, Russia; **RC,** Rubidge Collection, Wellwood, Eastern Cape, South Africa; **SAM,** Iziko South African Museum, Cape Town, South Africa.

Systematic palaeontology

Reptilia Laurenti, 1768
Parareptilia Olson, 1947
Acleistorhinidae Daly, 1969
Karutia gen. nov.

Type species. *Karutia fortunata*, sp. nov.

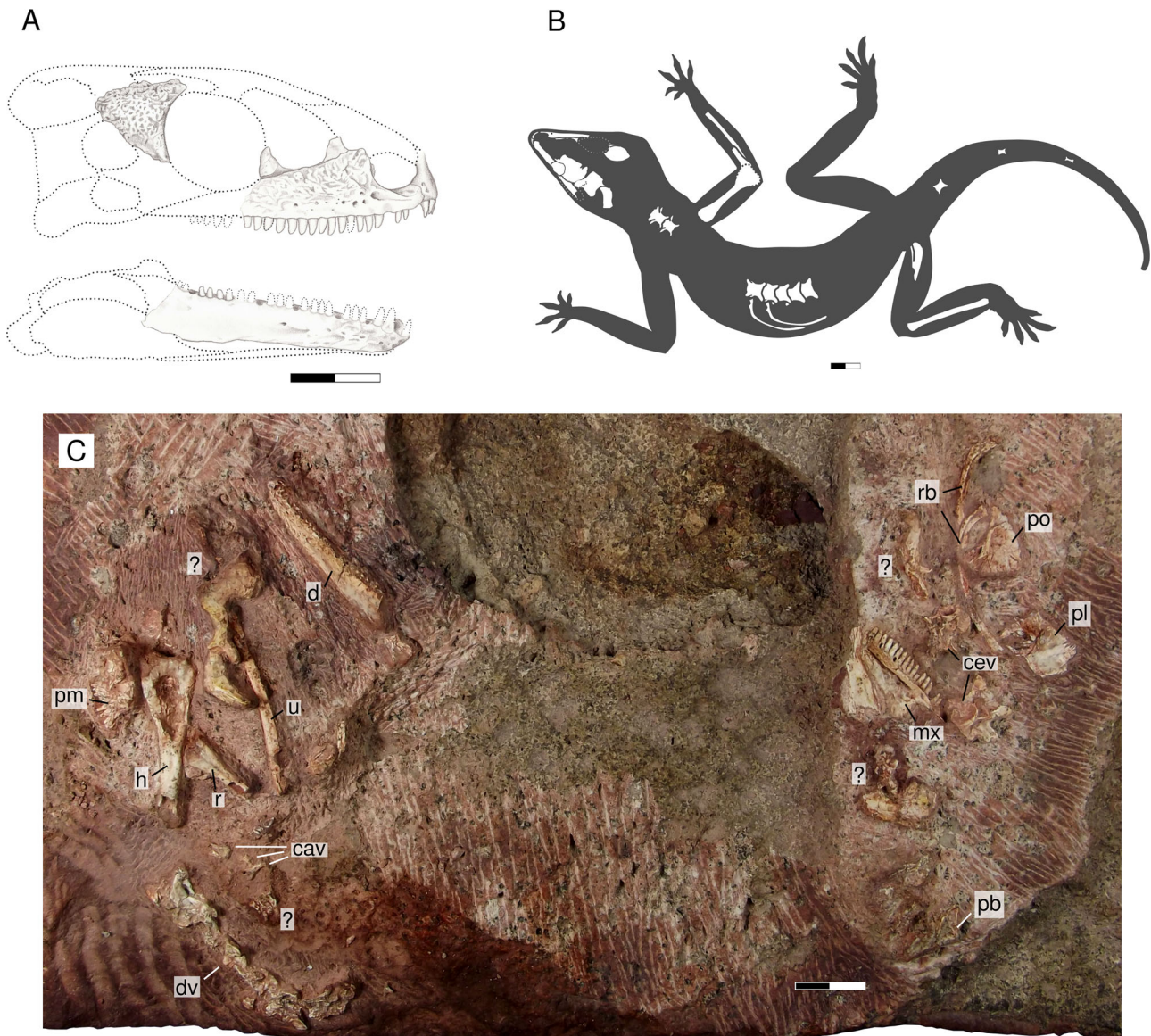**Diagnosis.** As for the type and only species.

Etymology. Derived from the word *kàruti* (skin covered by lumps or rugosities) in the native Timbira language, a reference to the cranial bone ornamentation.

Karutia fortunata sp. nov.
(Figs 1A–S, 2–5, 8)

Diagnosis. Small parareptile characterized by the presence of the following autapomorphies: (1) a wide,

Figure 1. *Karutia fortunata* gen. et sp. nov., MAP PV855, holotype. **A,** reconstruction of skull and mandible in lateral view. Missing bones based on *Delorhynchus cifellii* (*sensu* Haridy *et al.* 2016). **B,** skeletal reconstruction. **C,** skeleton embedded in matrix. **Abbreviations: cav,** caudal vertebra; **cev,** cervical vertebra; **d,** dentary; **dv,** dorsal vertebrae; **h,** humerus; **mx,** maxilla; **pb,** unidentified palatal bone; **pl,** palatine; **pm,** premaxillae; **po,** postorbital; **r,** radius; **rb,** ribs; **u,** ulna; **?,** unidentified bone. Scale bars equal 10 mm.

hemispherical postorbital boss covering most of the bone and overlaid by pits; (2) a rugose maxilla bearing homodont teeth with fluting on their lingual surfaces; and (3) a maxillary narial shelf in the form of a pocket that is hidden from lateral view by a wall. It can be distinguished from other members of Acleistorhinidae by having an oblique, straight dorsal margin of the maxilla, and by having three premaxillary incisiform teeth (shared with *Carbonodraco lundi*).

Etymology. The specific name derives from the Latin adjective *fortunatus* (lucky), a reference to the fortuitous

discovery of the fossil by CFK whilst the rest of the team was changing a flat tyre.

Type material. Specimen MAP PV855, a disarticulated skeleton comprising various cranial and postcranial bones.

Locality and horizon. Found in a mudrock paving quarry (MAP field number PB200; see Cisneros *et al.* 2020, fig. 1) in the Municipality of Nazária, 46 km SW of Teresina, Piauí State, Brazil. Unlike all other Pedra de Fogo tetrapods found in the area, which are preserved in massive, silicified mudstones of lacustrine

Table 1. Sources of information on parareptile taxa for comparisons and phylogenetic analysis. * indicates holotype.

Taxon	Literature	Specimens
Abyssomedon williamsi	MacDougall & Reisz 2014	
Acleistorhinus pteroticus	deBraga & Reisz 1996	*FMNH UR1038
Australothyris smithi	Modesto *et al.* 2009	
Belebey vegrandis	Reisz *et al.* 2007	
Barasaurus besairiei	Meckert 1995	SAM PK-K8275, SAM PK-K8282
Bashkyroleter bashkyricus	Tsuji *et al.* 2012	*PIN 164/3
Bashkyroleter mezensis	Tsuji *et al.* 2012	*PIN 162/30 PIN 3717/27
Bradysaurus baini	Lee 1997	SAM PK-K11638
Bolosaurus striatus	Watson 1954	
Carbonodraco lundi	Mann *et al.* 2019	
Colobomycter pholeter	Modesto 1999; Modesto & Reisz 2008; MacDougall *et al.* 2014, 2017	
Colobomycter vaughni	MacDougall *et al.* 2016	
Delorhynchus cifellii	Reisz *et al.* 2014; Haridy *et al.* 2016, 2017	
Emeroleter levis	Tsuji *et al.* 2012	
Erpetonyx arsenaultorum	Modesto *et al.* 2015	
Eudibamus cursoris	Berman *et al.* 2000	
Feeserpeton oklahomensis	MacDougall & Reisz 2012; MacDougall *et al.* 2019b	
Lanthanosuchus watsoni	deBraga & Reisz 1996	*PIN 271/1
Macroleter poezicus	Tsuji 2006	*PIN 3586/1, PIN 3717/32, PIN 4609-1
Mesosaurus tenuidens	Modesto 2006, 2010; Piñeiro *et al.* 2012; Laurin & Piñeiro 2017	
Microleter mckinzieorum	Tsuji *et al.* 2010	
Milleretta rubidgei	Gow 1972	*RC 14, RC 70, BP 1/2040
Nyctiphruretus acudens	Ivakhnenko 1979, 2008; Säilä 2010	
'Owenetta' kitchingorum	Reisz & Scott 2002	*BP/1/4195, BP/1/5398
Procolophon trigoniceps	Carroll & Lindsay 1985; deBraga 2003; Cisneros 2008	Various specimens at BP and SAM
Pareiasuchus nasicornis	Lee *et al.* 1997	SAM PK3016
Pareiasuchus peringueyi	Lee 1997	
Rhipaeosaurus tricuspidens	Ivakhnenko 2008; Tsuji *et al.* 2012	*PIN 164/2
Scutosaurus karpinskii	Lee 1997	PIN 2005/1883, 2005/1542

origin, the new specimen comes from an erosive-based fine-grained sandstone located at the top of the mudstone at a level of approximately 2.5 m in the exposed section (see the geological description in Cisneros *et al.* 2020). From the lower portion of the Pedra de Fogo Formation, Cisuralian.

Description

Most bones, with the exception of some vertebrae and palatal elements, were found disarticulated, and some elements in the slab could not be identified due to their fragmentary condition. The skull length is estimated at *ca*. 40 mm (based on comparisons with more complete acleistorhinid crania; Reisz *et al.* 2014; Haridy *et al.* 2016) and the whole skeleton at *ca*. 250 mm (Fig. 1). *Karutia fortunata* possesses extensive cranial sculpturing, although it is rather variable between bones, taking the form of sinuous rugosities and furrows, bosses of varying size and tiny pits. Most of the pits found in the

ornamentation of *Karutia fortunata* are irregularly shaped and differ from the circular pits found in *Acleistorhinus pteroticus* (deBraga & Reisz 1996), *Colobomycter* spp. (MacDougall *et al.* 2016, 2017), *Microleter mckinzieorum* (Tsuji *et al.* 2010) and the 'nycteroleters' (Tsuji *et al.* 2012). The cranial sculpturing in *Karutia fortunata* also contrasts with the pattern of shallow tubercles typical of millerettids (Gow 1972) or the honeycomb web of ridges and pits known in various captorhinids (Modesto 1998). There is no evidence of bony spines such as those found in procolophonids, pareiasaurs or *Lanthanosuchus watsoni*, although their absence is not certain given the incompleteness of the skull of *Karutia fortunata*.

Skull roof
Premaxilla. Both premaxillae (Fig. 2A–D) are preserved in articulation and are complete except for some damage to the palatal ramus and missing portions of the teeth. Their external surfaces are only lightly sculptured with shallow furrows. The premaxilla bears a vertical nasal
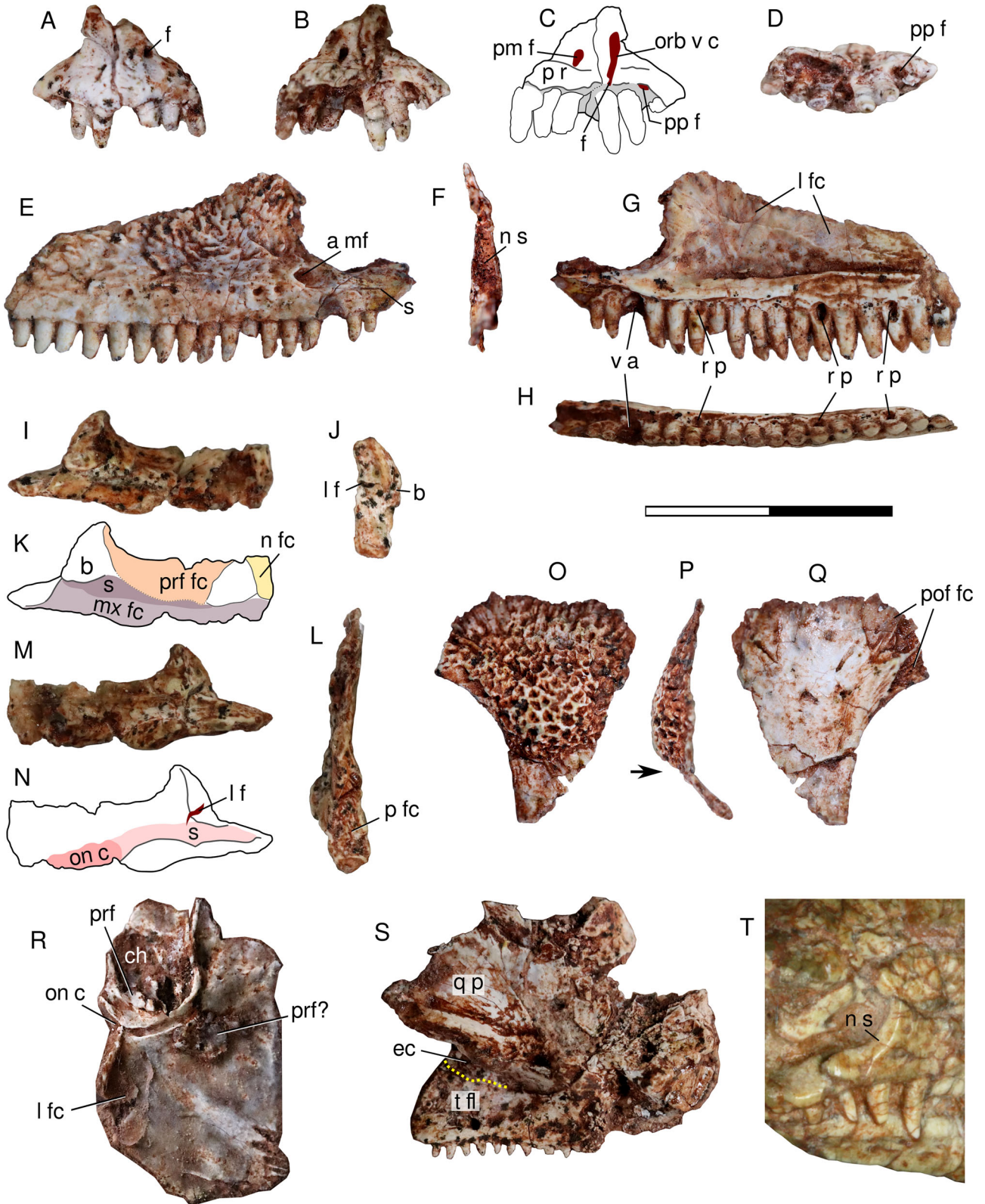
process that thins dorsally and is slightly curved posteriorly. The tip of this process, which would have contacted the nasal, is not preserved. A large recess above the level of the palatal ramus is visible in medial aspect; it is shaped like an inverted teardrop and likely corresponds to the posterior premaxillary foramen (Heaton 1979). This foramen perforates the palatal ramus, its passage being visible in the right maxilla through a transverse crack, and opens ventrally as a very small duct. A larger foramen is present below the palatal ramus, located between the second and the third tooth, which we identify as the ventral opening of the prepalatal foramen. The dorsal opening for the prepalatal foramen could not be located. It is probably minute and associated with the premaxillary foramen, as it is in *Captorhinus laticeps* (Heaton 1979), in which case it might be still covered by sediment. A circular opening preserved on the anterior surface of the right premaxilla, associated with the rim of the external naris, has not been reported in other parareptiles, although this area of the skull is seldom preserved or prepared. Judging by its location, this is likely the foramen for the orbitonasal vein (Heaton 1979). Considering its placement near the premaxillary foramen, it is probably connected to that foramen by a canal for the orbitonasal vein (Heaton 1979), exposed in the right premaxilla, which also served for passage of ophthalmic and ethmoidal nerves (Bellairs 1949). In contrast to most parareptiles, the premaxilla only makes a very modest contribution to the anterior portion of the ventral rim of the external naris.

The premaxilla of *Karutia fortunata* bears three incisiform teeth, a feature shared with *Carbonodraco lundi*. This is one fewer than the count estimated for *Acleistorhinus pteroticus* (deBraga & Reisz 1996), but one more than in both *Colobomycter* species (MacDougall *et al.* 2014, 2017). The premaxilla is damaged or absent in most *Delorhynchus cifellii* specimens, but this species was estimated to have four or five incisiforms by Reisz *et al.* (2014), although three or four seems more likely based on a well-preserved juvenile specimen (OMNH 77676, figured by Haridy *et al.* 2016; Y. Haridy, pers. comm.). The largest incisiform tooth of *Karutia fortunata* is the mesial-most. This tooth is slightly recurved lingually, with a sub-circular base, and its width is equal to roughly one-third of the basal-apical dimension. It progressively thins towards the labiolingually flattened crown apex. The second and third incisiforms are smaller versions of the first. Tooth implantation is pleurodont.

Maxilla. A right maxilla is preserved and has been prepared in both lateral and medial views (Fig. 2E–H). It is mostly complete (length = 17 mm), except for the missing jugal process and a few posterior teeth. Its lateral surface bears prominent sculpturing in the form of an array of rugosities and furrows. Sculpturing is coarser dorsally, becoming weaker ventrally along a 'belt' that runs anteroposteriorly, adjacent to the dentition. The boundary between the coarse and the weak ornamentation is punctuated by a row of supralabial foramina, a condition most closely resembling the maxilla of *Feeserpeton oklahomensis* (MacDougall & Reisz 2012, fig. 1d). In typical parareptilian fashion, the anterior maxillary foramen is distinctly larger than all other foramina (Laurin & Reisz 1995). This opening continues as a well-developed, anteriorly directed groove that borders much of the ventral rim of the external naris, similar to that of *Delorhynchus cifellii* and *Feeserpeton oklahomensis*, although this groove appears slightly oblique and anteroventrally oriented in the North American forms. This groove is, in turn, bordered ventrally by a much thinner sulcus that also originates from the anterior maxillary foramen (Fig. 2E), a feature also seen in *Delorhynchus cifellii* (Reisz *et al.* 2014, fig. 1b). In *Karutia fortunata*, this second sulcus continues anteriorly for most of the extension of the external naris, beyond the position of the first preserved maxillary tooth. As in most parareptiles, the maxilla bears a high anterodorsal process, which in *Karutia* forms the entire posterior margin of the external naris. The configuration of this process in the new taxon, however, differs from that in other acleistorhinids. In other members of the clade, the maxilla rises to form a prominent step that is located either anterior to the lacrimal (*Acleistorhinus pteroticus*) or over the lacrimal (*Colobomycter* spp., *Delorhynchus cifellii*, *Feeserpeton oklahomensis*),

Figure 2. *Karutia fortunata* gen. et sp. nov., MAP PV855, holotype. Skull roof and palatal bones. Premaxilla in **A,** anterior, **B** and **C,** posterior and **D,** ventral (slightly posterior) views. Right maxilla in **E,** lateral, **F,** anterior (focusing on the narial shelf), **G,** medial and **H,** occlusal views. Right lacrimal in **I,** lateral, **J,** posterior (slightly dorsal), **K,** lateral, **L,** ventral, and **M** and **N,** medial views. Left postorbital in **O,** lateral, **P,** anterior and **Q,** medial views. **R,** right palatine in dorsal view. **S,** left pterygoid and ectopterygoid in posteroventral view. **T,** anterolateral view of the left naris of *Acleistorhinus pteroticus*, showing the narial shelf. Scale bars: A–I, K–T equal 10 mm; J equal 6 mm. The arrow (in **P**) shows the step on the surface of the postorbital. **Abbreviations: a mf,** anterior maxillary foramen; **b,** boss; **ch,** choana; **ec,** ectopterygoid; **f,** foramen; **l f,** lacrimal foramen; **l fc,** lacrimal facet; **mx fc,** maxillar facet; **n fc,** nasal facet; **n s,** narial shelf; **on c,** orbitonasal canal; **orb v c,** orbitonasal vein canal; **p fc,** palatine facet; **p r,** palatal ramus; **pm f,** premaxillary foramen; **pof fc,** postfrontal facet; **pp f,** prepalatal foramen; **prf,** prefrontal fragments; **prf fc,** prefrontal facet; **q p,** quadrate process; **r p,** resorption pit; **s,** sulcus; **t fl,** transversal flange; **v a,** vacant alveolus. Photograph in **T** by William Simpson.

forming the posterior border of the anterodorsal process. In *Karutia fortunata* this step is absent; instead, the dorsal margin of the maxilla is straight and oblique, resembling the condition in millerettids (Gow 1972) and *Emeroleter levis* (Tsuji *et al*. 2012). A well-developed narial shelf for supporting the nasal capsule (*sensu* Reisz *et al*. 2014) is visible in anterior view (Fig. 2F). This takes the form of a vertically oriented, oval pocket that is ventrally wide and narrows dorsally. A delicate sheet of bone protruding anteriorly from the external surface of the maxilla prevents much of the shelf from being seen in lateral view. This configuration contrasts with other parareptiles, where the maxilla contributes to the narial shelf but is well exposed in lateral view, such as *Acleistorhinus pteroticus* (Fig. 2T), *Colobomycter* spp., *Delorhynchus cifellii*, *Procolophon trigoniceps* and *Nyctiphruretus acudens*. The narial shelf is also hidden from medial view by an inner bone lamina. The maxilla gently decreases in height along the suture with the lacrimal.

Seventeen maxillary tooth positions are present, but there should be at least five more in the missing posterior end that would occlude with their lower counterparts. In contrast to all other acleistorhinids except *Delorhynchus cifellii*, there is no distinct caniniform region. All maxillary teeth are long, conical and of comparable size, with crown apices slightly recurved posteriorly. In addition, the posterior-most teeth are gently curved inwards (Figs 2H, 3A). As in other acleistorhinids, maxillary tooth implantation is clearly pleurodont. Delicate, longitudinal striations are visible on the lingual surface of the base of each maxillary tooth (Fig. 3B), suggesting the presence of plicidentine. This condition is not common in parareptiles but has been reported in the acleistorhinids *Colobomycter* spp. (MacDougall *et al*. 2014, 2016), *Delorhynchus cifellii* (Reisz *et al*. 2014) and *Carbonodraco lundi* (Mann *et al*. 2019), and is also known in the South African millerettids (Gow 1972) and the Russian *Macroleter poezicus* (Tsuji 2006). In the genus *Colobomycter* and in *Macroleter poezicus*, however, fluting occurs on the labial side of the teeth as well. Four tooth replacement events are visible in lingual aspect, consisting of three resorption pits and one empty alveolus (Figs 2G, H, 3B).

Lacrimal. A complete right lacrimal is preserved (Fig. 2I–N). It is anteroposteriorly long, transversely wide posteriorly and gradually tapers towards its anterior end. Its lateral surface is sinuous and covered by depressions, grooves and small bosses. In lateral view, the posterior end appears as a wedge that lies over the palatine and laterally borders the orbit. From this wedge, the bone rises as a sigmoid contour that contributes to the anterior portion of the orbital rim. A small, anteroposteriorly oriented oval protuberance is present next to the rim, approximately at the mid-height of the bone. After reaching the dorsal-most point at the rim, the lacrimal slopes down, forming a large concavity that occupies half of the dorsal surface of the bone and represents the notch for a scarf joint with the prefrontal, in which the lacrimal is the lowermost bone. The lacrimal becomes thicker anteriorly, after its contact with the prefrontal, but thins again at its anterior-most end where it would lie below the nasal. A shallow, anteroposteriorly directed sulcus starts at the orbital rim and extends below the boss and the concave depression that accommodates the prefrontal, almost reaching the surface for articulation with the nasal. The sulcus is here regarded to represent the border of the scarf articular surface for the overlapping margin of the maxilla. It is possible that the prefrontal and the maxilla had a short sutural contact over the lacrimal, covering its lateral exposure over the mid-length, as the lacrimal becomes very thin at this point. The lacrimal would be exposed again more anteriorly where it thickens laterally, close to its contact with the nasal. If this interpretation is correct, the condition would be similar to that reported for *Delorhynchus cifellii*, where the lacrimal also has a double lateral exposure (Reisz *et al*. 2014).

In posterior view, the lacrimal appears nearly rectangular, having a sinuous lateral outline due to the sulcus that articulates with the maxilla and the boss located dorsally to this sulcus. The base of the bone shows some rugosities in this view, which may indicate a contact with the jugal. A vertical ridge along the dorsal half of the bone separates the lateral surface of the lacrimal from the anterior wall of the orbit. A lacrimal duct runs from the base of this ridge to the medial edge, where it connects with the orbitonasal canal. Above this duct, the orbit wall is medially inclined. In ventral view, the most prominent feature of the lacrimal is the surface for articulation with the palatine. It is slightly reniform, laterally convex and medially concave, being wider posteriorly and bearing rugosities. In medial view, a long, shallow parasagittal indentation runs anteriorly from the posterior wedge, extending over two-thirds of the bone. The posterior half of this sulcus is limited ventrally by a thickened platform that lies over the palatine. This shelf reaches the midpoint of the bone, progressively thickening and curving ventrally. The anterior half of the sulcus, just after the lacrimal-palatine suture, is not bounded ventrally by the lacrimal and represents the contribution of this bone to the lateral border of the orbitonasal canal. The lacrimal duct is also visible in medial view, where it appears to be connected to the orbitonasal canal through the aforementioned sulcus. Above the lacrimal duct, a dorsal process of the lacrimal
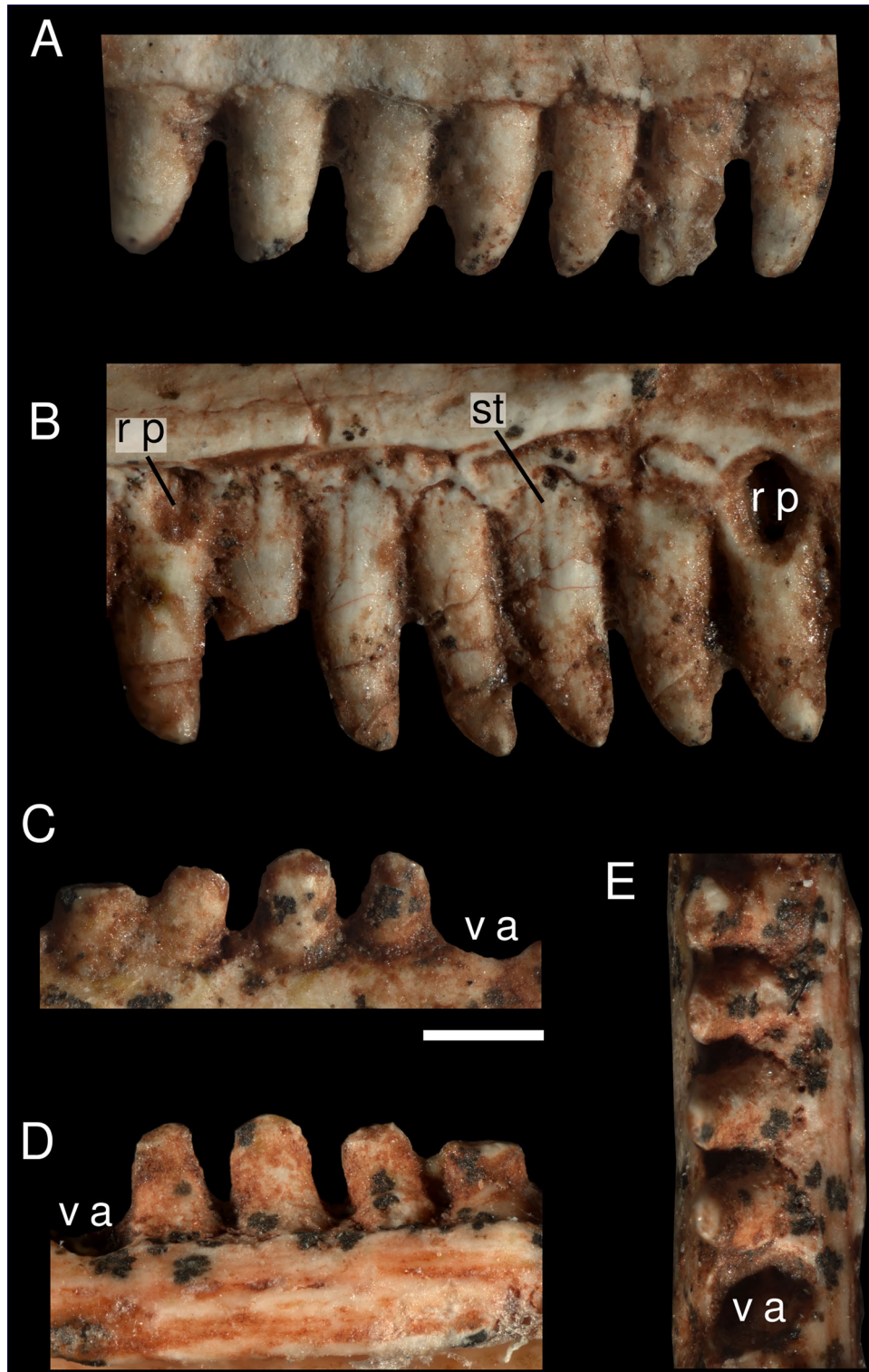
Figure 3. Dentition of *Karutia fortunata* gen. et sp. nov., MAP PV855, holotype. Right maxillary teeth in **A,** labial view (tooth positions 8–14) and **B,** lingual view (tooth positions 6–12). Posterior left dentary teeth (tooth positions 21–25) in **C,** lingual view, **D,** labial view and **E,** occlusal view (mesial to the top). **Abbreviations: r p,** resorption pit; **st,** striations; **v a,** vacant alveolus. Scale bar equals 1 mm. Photographs by Katia Piovesan. ©[Katia Piovesan]. Reproduced by permission of Universidade Federal do Pernambuco.

rises as a pyramidal structure, consisting of a posterior face that forms the orbit wall and an anteromedial face that represents the surface for articulation of the prefrontal. A recurved sulcus that borders the anteromedial face likely represents the ventral border of the prefrontal contact.

Postorbital. A complete left postorbital is preserved (Fig. 2O–Q). In lateral view, this bone is essentially triangular, having distinct dorsal, anterior and posteroventral margins. Most of the bone is covered by an ornamentation consisting of minute (less than 1 mm wide) irregular pits, resembling the skull roof sculpturing of *Colobomycter* spp. and *Emeroleter levis*. The most remarkable feature of the postorbital, however, is a large boss that covers most of its lateral surface. At the dorsal portion of the bone, this bump rises smoothly, being at its midpoint nearly 5 times thicker than other parts of the bone, giving the postorbital a swollen outline in anterior and posterior views. The ventral ramus of the postorbital bears a step that marks the ventral edge of the boss, below which the bone thins and continues, nearly devoid of ornamentation, as an acute process that bordered the orbit and likely shared a contact with the jugal. The anterior edge of the bone is concave, forming the posterodorsal portion of the orbital rim. This edge is thickened, forming an arched bar that is visible in medial view. The posteroventral margin of the postorbital is thin and slightly sinuous. These notches indicate sutures with the supratemporal and jugal, but the extent of these contacts is difficult to assess because the sinuosity becomes more subtle at the middle of the postorbital, where it could represent the edge of a temporal opening. The dorsal and posterodorsal borders of the postorbital are highly notched, indicating serrated sutures with the parietal and with the supratemporal. The inner surface of the postorbital is slightly concave and smooth overall, with some small foramina and sparse furrows. On its anterodorsal corner it bears two triangular depressions that represent sutural contacts. Judging from their placement in the bone, both presumably represent surfaces for scarf joints with the postfrontal.

The postorbital of *Karutia fortunata* resembles the same element in *Delorhynchus cifellii*, where a bossed postorbital also has a step over its ventral ramus (Reisz *et al.* 2014, fig. 3c). The postorbital in the Russian nycteroleters is thickened and ornamented and also bears a prominent step, although it is not located over the ventral ramus but along the posteroventral edge, where it forms the rim of the wide temporal notch (Tsuji 2006; Müller & Tsuji 2007; Tsuji *et al.* 2012). The absence of the latter condition in *Karutia fortunata* suggests that a temporal notch was either absent or small.

Palate

Palatine. A left palatine was found dorsally exposed (Fig. 2R). It is nearly complete, missing only a small portion of its posteromedial border. It is a thin, sub-rectangular bone with nearly parallel medial and lateral margins and a large anterolateral notch. Three-quarters of its medial border is straight, showing that most of its contact with the pterygoid was in the form of a butt suture. The posterior-most quarter of the medial border, however, is notched, showing a serrate contact with the pterygoid. The missing area of the palatine was presumably a small fragment that contacted the pterygoid medially and the ectopterygoid posteriorly. The portion of the posterior margin that is not damaged consists of an oblique, posteromedially directed uniform contour, which likely contacted the ectopterygoid. The lateral border is slightly damaged on its posterior-most edge, but the anterior part preserves a low, thin ridge that would have lain against the maxilla. Medial to the lateral border, there is an oval scar that represents the articular facet of the overlying lacrimal. A shallow sulcus originates from the anterior point of this suture and extends posterolaterally to the serrated palatine-pterygoid contact. This oblique groove presumably represents the dorsal exposure of a ventral tooth-bearing ridge that would continue towards the pterygoid, which is the primitive condition for parareptiles. Small fragments of bone, probably remains of the prefrontal, are found attached anterior to this sulcus, approximately at the centre of the palatine. The anterolateral portion of the bone forms a large notch that constitutes the posterior and posteromedial margins of the choana. The rim of the choana is formed by a ridge, which is in turn bordered by sulci. A suture is visible along the posterior portion of the rim, perforated by small foramina, and the small portion of bone still attached to it is regarded as the remains of the prefrontal. Tiny, disarticulated fragments of bone inside the choana may represent portions of the missing prefrontal as well. The ridge of the choana is bordered by a thin but well-defined, recurved sulcus that represents the palatine contribution to the orbitonasal canal. This sulcus becomes deeper along the posterior border of the choana, where it passes anterior to the facet for the palatine and continues anteriorly as a duct formed by both bones, and likely also by the prefrontal. A second, shallower sulcus is present between the main sulcus and the ridge that borders the choana. This second groove is smaller, being restricted to the posterolateral margin of the choana, but presumably also continued anteriorly into the orbitonasal canal. The orbitonasal canal is formed, therefore, by a double sulcus, a condition that is also seen in procolophonids (Carroll & Lindsay 1985; Hamley *et al.* 2020). No suborbital
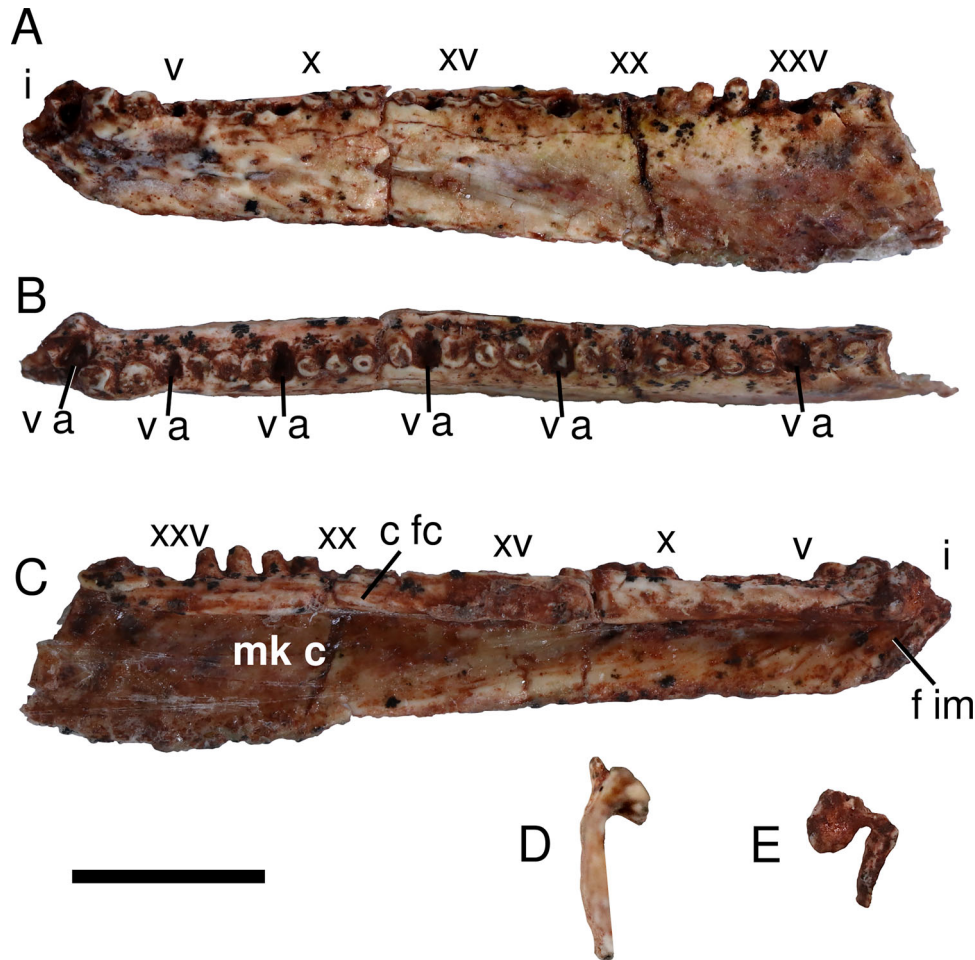
Figure 4. *Karutia fortunata* gen. et sp. nov., MAP PV855, holotype. Left dentary. **A,** lateral view, **B,** occlusal view, **C,** medial view **D,** posterior view and **E,** symphysis in medial view (occlusal surface to the top). **Abbreviations: c fc,** coronoid facet; **f im,** foramen intermandibularis medius; **mk c,** Meckelian canal; **v a,** vacant alveolus. Roman numerals indicate tooth positions. Scale bar equals 5 mm.

foramen was recognized, confirming the absence of this feature in members of the Acleistorhinidae (MacDougall *et al.* 2019b).

Pterygoid. One partial left pterygoid (Fig. 2S) is preserved. It consists of the transverse wing, exposed in dorsal view and partly overlain by a flat bone that is tentatively interpreted as the quadrate process of the same pterygoid, which has collapsed and now lies exposed in medial view. The quadrate process, in turn, was covered by the aforementioned palatine. The pterygoid transverse flange has a smooth dorsal surface, its posterior margin being nearly straight and slightly concave. At least nine teeth can be recognized along this border. These are sub-equal in size, conical and oriented posteroventrally. The preserved portion of the putative quadrate process is devoid of major features except for a thickened ventral ridge. The pterygoid is associated with other, fragmentary bones of uncertain identification.

Ectopterygoid. A sinuous suture visible on the anterior portion of the pterygoid transverse flange in dorsal view is here considered to represent the pterygoid contact with the ectopterygoid (Fig. 2S). The medial portion of this suture is transversely oriented, after which it curves anterolaterally. The exposure of the ectopterygoid in this view is limited due to the overlying pterygoid quadrate process, confirming the presence of this bone but precluding any further description.

Mandible

Dentary. A nearly complete left dentary is present (Fig. 4). In lateral view, it is covered by ornamentation of rugosities and furrows resembling those in the maxilla, but more shallow and concentrated towards the anterior end of the mandible. This region of the dentary also is perforated by a series of foramina, the largest of which is located below the fifteenth tooth position. The dentary becomes more robust towards the symphysis as

the cavity for the Meckelian cartilage narrows anteriorly into a slender canal. Mirroring the maxilla, these foramina are loosely aligned parallel to the level of the occlusal margin of the bone.

At least 28 tooth positions are preserved, a higher count than in *Carbonodraco lundi* (24; Mann *et al.* 2019) and *Feeserpeton oklahomensis* (25; MacDougall *et al.* 2019b) but matching the number recorded in *Delorhynchus cifellii* (Reisz *et al.* 2014). Most teeth are broken or missing. There appears to be a small, damaged tooth base at the beginning of the tooth row. This is followed by a much wider, empty alveolus and two broken teeth that are equivalent in width to the latter. These three teeth are the largest in the dentary. The alveoli for the first four teeth are arranged in a curved, slightly sigmoid row at the symphysis, which protrudes labially at the third and four position. The tooth row continues as a straight line from the fifth tooth position to the last. It can be observed, in occlusal view, that the straight portion of the tooth row is not aligned with the main axis of the dentary but instead is oblique in relation to it, resulting in the mesial-most teeth being close to the labial wall and the distal-most teeth bordering the lingual wall. The best-preserved teeth are located in the posterior region of the dentary and are mainly conical and shorter than their upper counterparts (Fig. 3C–E). They are also proportionally shorter than in other acleistorhinids where this area is visible. Their bases are elliptical, being slightly narrower mesodistally than labiolingually. The posterior teeth are angled obliquely, some 110° from the occlusal surface of the dentary, resulting in a dorsolabially oriented tooth axis. They lack the posteriorly recurved apex present in the maxillary teeth. There is evidence of tooth replacement in the dentary. Six empty sockets are present, located at the second, fifth, ninth, fourteenth, eighteenth and twenty-fifth tooth positions (Fig. 4B), indicating the typical reptilian pattern of alternating replacement waves, in contrast to the derived and highly synchronous tooth replacement of bolosaurid parareptiles (Snyder *et al.* 2020).

In contrast to the upper marginal teeth, the lower dentition is not pleurodont. The tooth roots are not visible and the bases of the exposed portions of the teeth are limited lingually by a continuous sulcus which in turn is bordered by a lingual wall that is shallower than the labial wall (Fig. 3E). The lower dentition thus appears to exhibit the pleuroacrodont pattern of tooth implantation, as also reported for *Delorhynchus cifellii* (Haridy *et al.* 2016).

The cavity for the Meckelian cartilage is fully exposed in lingual view. It is tall posteriorly and gradually thins anteriorly towards the symphysis, where it opens as a foramen intermandibularis medius. The cavity is bordered dorsally by a shelf that shows rugosities and slightly sinuous, longitudinal grooves that evince the coronoid articular facet. This sutural surface extends from the posterior end of the dentary to at least as far as the mid-length of the bone, at the seventeenth tooth position, but it could extend farther anteriorly because a small area here is still covered by matrix. It is not possible to determine whether there was one coronoid as in *Feeserpeton oklahomensis* (MacDougall *et al.* 2019b) or two coronoids as in *Delorhynchus cifellii* (Haridy *et al.* 2017). The second hypothesis, however, is more likely, taking into consideration that the coronoid articular facet in *Karutia fortunata* is comparable in extent to that of *Delorhynchus cifellii* and much longer than in *Feeserpeton oklahomensis*. Anterior to the thirteenth position, the shelf is devoid of rugosities or grooves and becomes more convex, indicating that no bone covered this area and the dentary was exposed medially as it approached the symphysis. The dentary symphysis has the shape of an inverted 'U' that has been slightly rotated clockwise, with a dorsoventrally shorter, but transversely wider lingual wall and a thinner, dorsoventrally higher labial wall.

Axial skeleton

Our knowledge of acleistorhinid postcrania is currently restricted to the recent description of an anterior portion of the skeleton of *Delorhynchus cifellii* and a few vertebrae, a scapula and a phalanx of *Colobomycter vaughni* (Reisz *et al.* 2014; MacDougall *et al.* 2016). Therefore, the skeleton of *Karutia fortunata* is an important addition to the knowledge of the postcranium in this clade.

Vertebrae. Seven presacral vertebrae were recognized (Fig. 1C). Two of them were found disarticulated, located between the maxilla and some palatal bones; they were detached from the matrix and fully prepared. These vertebrae suffered from compaction during diagenesis, with dorsoventral flattening in one case (Fig. 5A, B; anteroposterior length = 6.2 mm) and lateral compression in the other (Fig. 5A–C; anteroposterior length = 6.3 mm). The latter has also lost the right prezygapophysis, exposing some of the neural canal. Apart from this damage, both vertebrae are well preserved. A string of five articulated dorsal vertebrae of larger dimensions (Fig. 1C; anteroposterior length ~7.5 mm) is located near the humerus. These were prepared in dorsal view, but their preservation is too poor to provide an accurate morphological account. Therefore, the description will be based on the two disarticulated vertebrae, which are here considered to be cervicals based on their smaller size and slenderness,

Figure 5. *Karutia fortunata* gen. et sp. nov., MAP PV855, holotype. Postcrania. Cervical vertebra in **A,** dorsal and **B,** ventral views. Cervical vertebra in **C,** right lateral, **D,** left lateral and **E,** posterior views. **F,** caudal vertebrae and other indeterminate bones. **G,** proximal portion of ribs in posterior aspect. **H,** humerus in posterior view. **I,** partial radius (anterior or posterior view). **J,** ulna in anterior view. Left femur in **K,** proximal (dorsal aspect to the top), **L,** dorsal, **M,** ventral and **N,** anterior views. Left fibula in **O,** posterior, **P,** anterior and **K,** lateral views. **Abbreviations: cv,** caudal vertebrae; **dp c,** deltopectoral crest; **it f,** intertrochanteric fossa; **in t,** internal trochanter; **ph,** phalanges; **pk,** pocket; **n c,** neural canal; **r,** ridge; **t v,** transverse process. Scale bar equals 10 mm.

which is consistent with the cervical vertebrae in *Emeroleter levis* (Tsuji *et al.* 2012).

The dorsal spines are relatively low, but higher than in *Emeroleter levis* (Tsuji *et al.* 2012). They have a somewhat robust base and are strongly inclined posteriorly, resembling the pattern known in millerettids, *Delorhynchus cifellii* and some procolophonids (Gow 1972; Reisz & Scott 2002; Cisneros & Schultz 2003; Säilä 2008; Reisz *et al.* 2014). The neural arches are well ossified and fused to the pleurocentra, confirming the mature status of this individual. The vertebrae exhibit the classical parareptilian feature of a moderate swelling of the zygapophyses, albeit to a lesser degree than what is seen in procolophonoids or pareiasauromorphs. A lateral, oblique ridge extends from the postzygapophysis anteroventrally towards the transverse process. This ridge is fairly well developed and akin to the vertebrae of *Delorhynchus cifelli* and *Colobomycter pholeter* but is moderate in comparison to the extreme condition seen in pareiasaurs (Boonstra 1934). An oval depression extends parallel to the ventral edge of this ridge. This structure is present in *Delorhynchus cifellii* and *Colobomycter pholeter* and is homologous with the well-developed lateral pocket that is present in various parareptiles (Reisz *et al.* 2014). A short, delicate transverse process is visible on the left side of one of the cervicals (Fig. 5A, B). The vertebrae have pinched centra, creating a ventral keel. This keel is thin in ventral view, moderately concave in lateral view, and extends through most of the length of the centrum. The centra were not fully cleaned due to their fragility, but they are strongly amphicoelous and it is very likely that they are notochordal. The morphology of the centra is compatible with the presence of small intercentra, although these were not found.

Three disarticulated caudal vertebrae were found near the string of thoracic vertebrae (Fig. 5F). All that can be said is that they are simplified and mainly featureless, one of them being a mere cylindrical centrum. Other nearby small bones may represent additional caudals, but their preservation is not sufficient to allow a confident identification.

Ribs. Two ribs were found next to the postorbital bone (Figs 1C, 6G). One of the ribs, which is partially covered by the other, preserves most of the head. The second rib, although missing its proximal end, is better exposed and was fully prepared in this aspect, complementing the information from the rib that lies below it. They are long, arched and of fairly conservative appearance. The estimated total length of a complete rib is equivalent to four dorsal vertebrae. This is proportionally longer than the mid-dorsal rib length of *Emeroleter levis* and *Nyctiphruretus acudens*, which is equivalent to

three dorsal vertebrae (Efremov 1940; Tsuji *et al.* 2012), but comparable to the bolosaurid *Eudibamus cursoris*, although the latter possesses vertebrae that are unusually short anteroposteriorly (Berman *et al.* 2000). Despite some subtle separation between capitulum and tuberculum in the form of a dorsal concavity, the rib head is essentially holocephalous. A prominent sulcus is present, similar in this respect to *Emeroleter levis*, where this feature is visible along the posterior aspect of the ribs (Tsuji *et al.* 2012). This sulcus is present throughout most of the rib extension in *Karutia fortunata* but is more prominent proximally, where it divides the rib into a dorsal, anteroposteriorly wider, shelf-like portion and a ventral, anteroposteriorly thinner portion.

Limbs

Humerus. For descriptive purposes, the postcranium is considered to be arranged having the epipodia in a horizontal plane, perpendicular to the body midline, and the propodia in a vertical plane. A partial right humerus is present (Fig. 5H), being fairly well preserved except for portions of the distal head. Its posterior surface was prepared but not removed from the block. The humerus of *Karutia fortunata* is noticeably more robust than in *Emeroleter levis* (Tsuji *et al.* 2012) but less than in *Procolophon trigoniceps* (deBraga 2003). It is not possible to compare its proportions with *Delorhynchus cifellii*, the only other acleistorhinid for which a humerus is known (Reisz *et al.* 2014), because the bones are exposed in different views. Flaring of the proximal humeral head is moderate: its maximum width is 2.9 times the minimum width of the shaft (by comparison, this ratio is 3.5 times in *Procolophon trigoniceps*; deBraga 2003). The deltopectoral crest appears relatively low. As exposed, the facet for the glenoid appears mostly straight along its proximal edge, gently curving on its dorsal margin where it becomes a low flange of bone. The distal head is not well exposed and has lost some of its anterior surface and apparently portions of the articular facet.

Radius. The proximal portion of a radius is present (Fig. 5I). Taking into consideration the dimensions of the nearby ulna (see below) and its proximity to the humerus, the preserved bone probably represents one-third of a right radius. It was left in the matrix and prepared in an aspect that could represent either anterior or posterior view. The facet for the radial condyle of the humerus is slightly damaged. Little can be said of this bone apart from the fact that it is gracile, its proximal head is moderately flared (equivalent to 2.37 times the width of the shaft), and it has a sulcus aligned with the
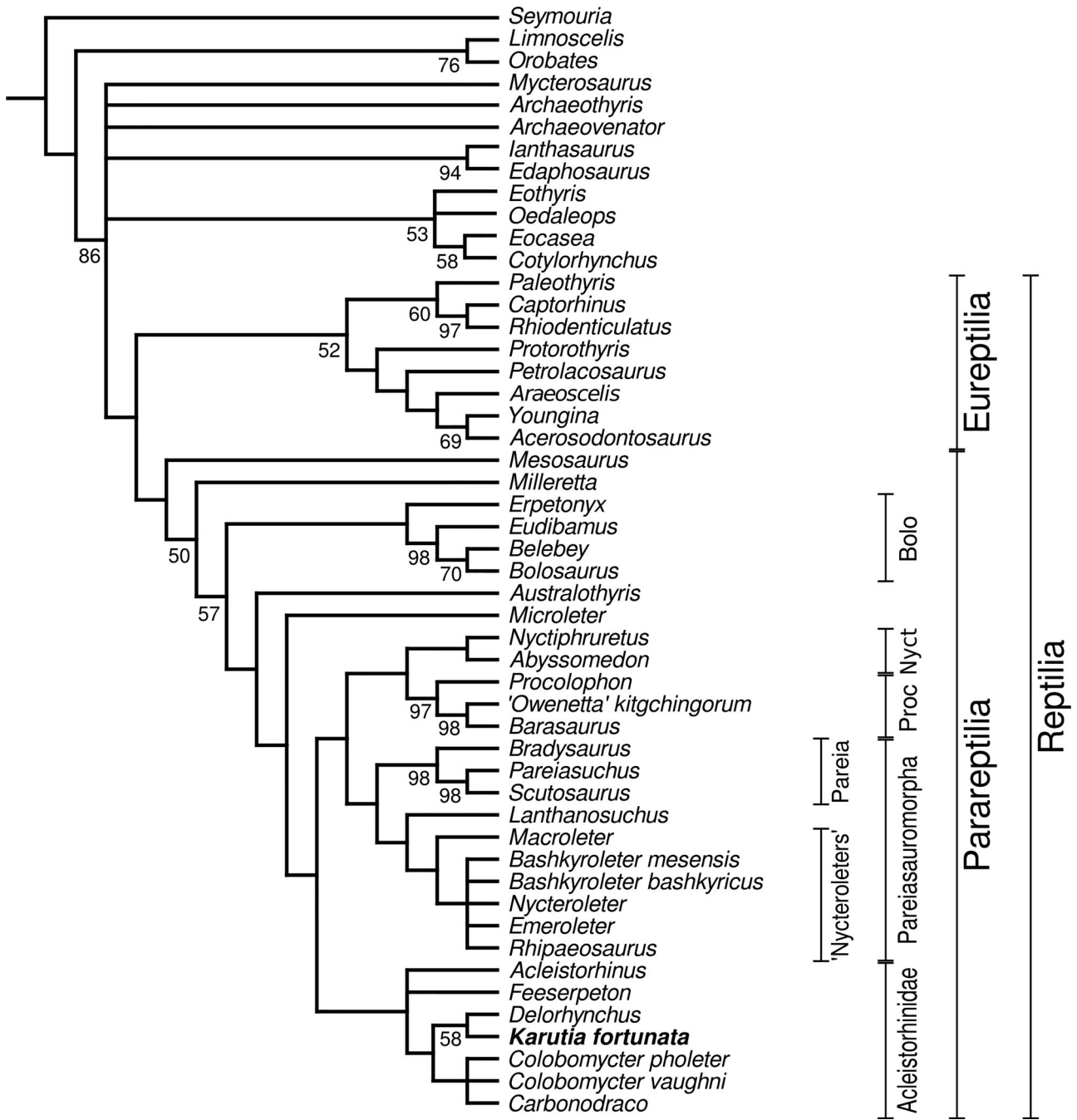
Figure 6. Strict consensus of 40 most parsimonious cladograms of parareptile relationships (length 700 steps). Symmetric resampling values (≥50%) are provided before the nodes. **Abbreviations: Bolo,** Bolosauridae; **Nyct,** Nyctiphruretidae; **Pareia,** Pareiasauria; **Proc,** Procolophonoidea.

long axis of the bone that becomes deeper towards the shaft as the bone thins.

Ulna. A nearly complete ulna is present (Fig. 5J) and although it is missing both proximal and distal ends, it is fairly well preserved. Judging from its proximity to the humerus, it is probably a right ulna. It was left within the matrix and prepared in what is here considered the anterior aspect. The bone is quite long and slender, measuring at least 25.9 mm in length (equivalent to four dorsal vertebrae) against a width of 1.38 mm at the mid-shaft in proportions that resemble the ulna of *Emeroleter levis* (Tsuji *et al.* 2012). The ulna is slightly arched, being medially concave and laterally convex. A

short sulcus, shallower than the one present in the radius, is visible along its proximal head. This sulcus is aligned with the long axis of the bone and widens proximally, but its total extent cannot be assessed due to damage in this region.

Femur. The proximal portion of a left femur is preserved (Fig. 5K–N). It was detached from the matrix and fully prepared. The main visible feature is a long intertrochanteric fossa, which in turn suggests that the bone was much longer than the recovered fragment. This fossa is bordered anteriorly by a well-developed, elongate internal trochanter. This trochanter initially extends parallel to the anterior edge of the bone but becomes oblique distally. Both the fossa and the internal trochanter are incomplete, missing their distal ends. In both anterior and posterior views the femur appears very thin, but this may be in part a result of compression during diagenesis, as is seen in other bones of the specimen. In dorsal aspect the femur is mostly featureless, having some damage near the articular surfaces. The elongated intertrochanteric fossa and the internal trochanter, together with the overall slenderness of the bone, contrast with most known parareptiles, but strongly resemble the morphology of the femur in *Emeroleter levis* (Tsuji *et al.* 2012).

Fibula. A nearly complete fibula is present (Fig. 5O–Q), here considered to be from the left hind limb due to its proximity to the left femur. It is only missing a small portion of the proximal articulation. It was detached from the block and for the most part prepared, except for some sediment left on the distal facet to maintain stability. Like the ulna, the fibula is greatly elongated and gracile, resembling the same element in *Emeroleter levis*, *Eudibamus cursoris* and the eureptile genus *Araeoscelis* (Reisz *et al.* 1984). Its minimum length is 28.5 mm, its mediolateral and anteroposterior dimensions at the shaft are 2.5 mm and 1.5 mm, respectively. The fibula is visibly arched, as in most early amniotes. In anterior view, a shallow deltoid notch is present over the proximal head. A short sulcus runs along the long axis of the bone before reaching the distal head, after which the head flares delicately and ends as a flat, spatulate projection. In posterior aspect, the proximal head bears a long 'V'-shaped depression, and a thin sulcus that runs along the medial margin of this depression. The remainder of the bone is mainly featureless in this view.

Phalanges. Small, partially disarticulated, bony elements found in the proximity of caudal vertebrae could represent phalanges (Fig. 5F), but their preservation is too incomplete to confirm this identification.

Discussion

Phylogenetic analysis

The cladistic analysis recovered a total of 40 most parsimonious trees (MPTs), all of which include a monophyletic Parareptilia. In the strict consensus tree (Fig. 6), *Karutia fortunata* is placed within Acleistorhinidae as the sister taxon of *Delorhynchus cifellii*. This relationship is well supported (symmetric resampling value 58). Synapomorphies shared between these taxa are the absence of size-related heterodonty on the maxilla (Character [ch.] 35:1), the presence of circumorbital tubercles (ch. 54:1) and the lack of a premaxillary contribution to the ventral margin of the external naris (ch. 178:1). The clade Acleistorhinidae is diagnosed by seven synapomorphies: a frontal lateral lappet (ch. 5:1); maxilla-quadratojugal contact (ch. 31:0); size-related heterodont dentition present in the maxilla (ch. 35:0); quadrate ramus continuous with transverse flange forming a ridge (ch. 72:1); paroccipital process oriented obliquely in relation to the horizontal plane of the skull (ch. 89:1); basioccipital/parasphenoid ventral exposure restricted to condylar region (ch. 97:1); and a single enlarged anterior vomerine tooth (ch. 167:1).

Carbonodraco lundi falls within Acleistorhinidae, corroborating the findings of Mann *et al.* (2019). *Carbonodraco lundi* is here recovered in a trichotomy with both species of the genus *Colobomycter*, a clade supported by the unambiguous synapomorphy of a greatly enlarged premaxillary tooth (ch. 178:1). An interesting result of the phylogenetic analysis is the placement of *Lanthanosuchus watsoni* within Pareiasauromorpha, as the sister taxon of *Macroleter poezicus* and the 'nycteroleters', rather than as a close relative of acleistorhinids. This relationship is supported by five synapomorphies: the presence of a quadratojugal anterior margin that does not reach the level of the posterior border of the orbit (ch. 40:1); a transversely broad basioccipital (ch. 96:0); an orbit that is exposed predominantly dorsally (ch. 184:2); a postfrontal posterior border located at the level of the pineal foramen (ch. 185:1); and a spine-like posterolateral edge of the skull roof (ch. 187:0).

Parareptile interrelationships and taxonomic remarks

Acleistorhinidae was proposed as a family-level taxon by Daly (1969), within the superfamily Procolophonoidea, to accommodate the reptile *Acleistorhinus pteroticus* from the Cisuralian of Oklahoma. Modesto (1999) expanded the composition of Acleistorhinidae to include the bizarre reptile *Colobomycter vaughni*, also from the Cisuralian of Oklahoma, previously regarded as either a basal synapsid
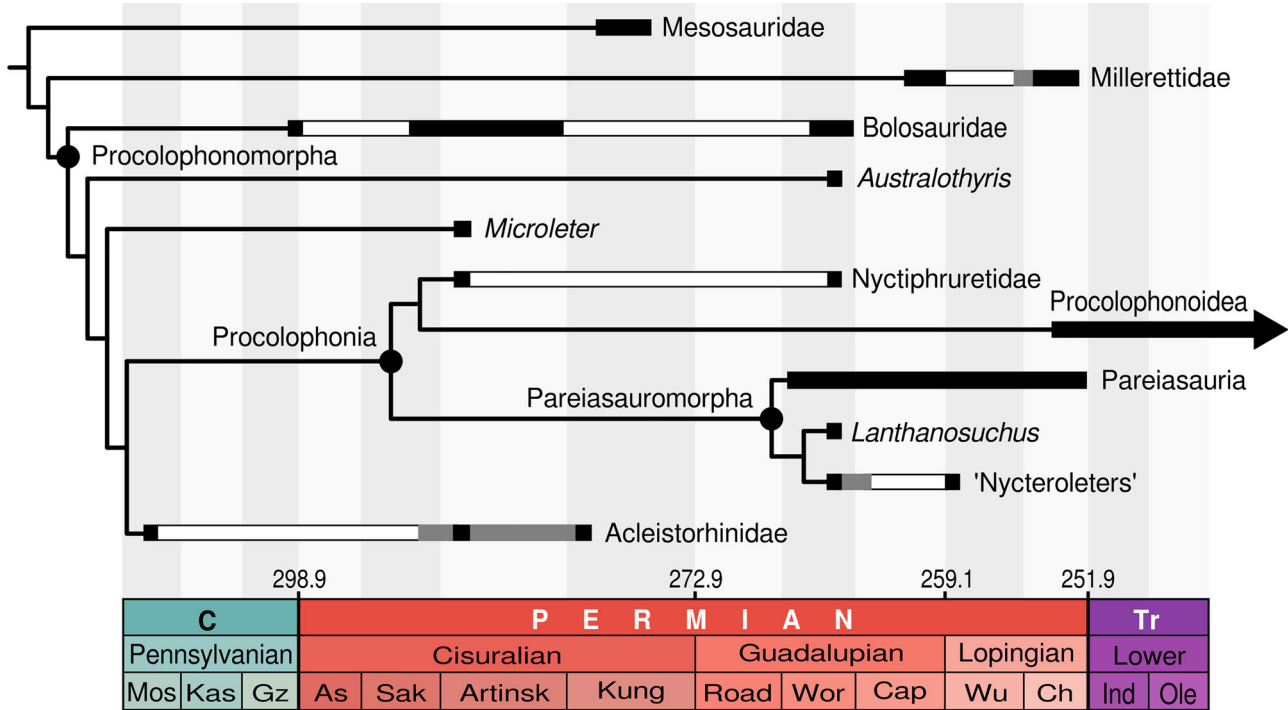
Figure 7. Stratigraphically calibrated strict consensus cladogram of the main parareptile groups. Known ranges, uncertain ranges and ghost lineages are represented by black, grey and white bars, respectively. **Abbreviations: Artinsk,** Artinskian; **As,** Asselian; **C,** Carboniferous; **Cap,** Capitanian; **Ch,** Changhsingian; **Gz,** Gzhelian; **Ind,** Induan; **Kas,** Kasimovian; **Kung,** Kungurian; **Mos,** Moscovian; **Ole,** Olenekian; **Road,** Roadian; **Sak,** Sakmarian; **Tr,** Triassic; **Wor,** Wordian; **Wu,** Wuchiapingian.

(Vaughn 1958) or a protorothyridid eureptile (Laurin & Reisz 1989). A close relationship between *Acleistorhinus pteroticus* and the enigmatic Russian parareptile *Lanthanosuchus watsoni* has been accepted since their inclusion in a cladistic analysis by deBraga & Reisz (1996), together forming the higher level taxon Lanthanosuchoidea. This group, and the family Lanthanosuchidae, were originally proposed by Efremov (1946) to accommodate the enigmatic tetrapods *Chalcosaurus rossicus*, *Lanthaniscus efremovi* and *Lanthanosuchus watsoni* from the Guadalupian of Russia, all characterized by broad, flat, heavily ornamented skulls with large temporal openings. Subsequent analyses derived from the description of new acleistorhinid specimens or taxa generally supported a relationship between the genus *Lanthanosuchus watsoni* and acleistorhinids. As a result, the name Lanthanosuchoidea Efremov, 1946, which has priority over Acleistorhinidae Daly, 1969, has been used either for a clade more inclusive than the latter or as a senior synonym, depending on the placement of *Lanthanosuchus watsoni* as basal to other acleistorhinids or more deeply nested within the clade (Modesto & Reisz 2008; MacDougall *et al*. 2014, 2016, 2017; Reisz *et al*. 2014; Modesto *et al*. 2015; Haridy *et al*. 2017).

A close relationship of the Lanthanosuchidae (*sensu* Efremov 1946) with pareiasaurs was reported in a cladistic analysis by Lee (1995). That phylogenetic analysis, however, did not include *Acleistorhinus pteroticus* and employed some taxa as outgroups that are currently considered to be nested within Parareptilia, such as bolosaurids, mesosaurids and millerettids.

The placement of *Lanthanosuchus watsoni* with the Russian 'nycteroleters' rather than with the acleistorhinids in this study was not triggered by adding *Karutia fortunata* or *Carbonodraco lundi* in the matrix, because running the analysis without both acleistorhinids does not affect its relationships. Rather, this novel relationship results from both the review of previous scores (on characters 5–7, 9, 15, 22, 25, 27, 35, 41–46, 51, 56, 58, 61, 64, 65, 67, 69, 72, 75, 76, 80, 81, 96, 125, 167, 169 and 173) and the inclusion of new characters in the data matrix (177–190). The cranial bauplan of acleistorhinids contrasts with that of *Lanthanosuchus watsoni* in many ways, such as placement of the orbits (laterally vs dorsally), geometry of the occiput and snout proportions, which are expressed in the new characters.

The grouping of *Lanthanosuchus watsoni* with the nycteroleters (including *Macroleter*) rather than with acleistorhinids is more congruent stratigraphically. All known acleistorhinids predate the Guadalupian (Fig. 7). On the other hand, with the exception of the nycteroleter specimen from the Chickasha Formation in Oklahoma, which could

be either late Cisuralian or early Guadalupian (see Reisz & Laurin 2001, 2002; Lucas 2002, 2017), all nycteroleter records are of Guadalupian–early Lopingian age (Cisneros & Tsuji 2009; Tsuji *et al.* 2012). The genus *Acleistorhinus pteroticus* is of early Kungurian age, whereas *Lanthanosuchus watsoni* is of Wordian age. Therefore, a ghost lineage of nearly 15 Ma that was present between these genera is eliminated in this study. Another long ghost lineage persists within Acleistorhinidae, however, due to the recent recognition of *Carbonodraco lundi* from the Pennsylvanian of Ohio, USA. This taxon, the oldest known parareptile, is separated from the Richards Spur acleistorhinids by a gap that spans the Moscovian to the Artinskian (Fig. 7). This ghost lineage may be partially reduced if the Pedra de Fogo Formation is correlated with the Chemnitz Petrified Forest in Germany (see discussions in Iannuzzi *et al.* 2018; Cisneros *et al.* 2020), which would result in *Karutia fortunata* being present in the late Sakmarian, but additional data are needed to confirm the age of the Pedra de Fogo Formation. In addition, the recovery of *Lanthanosuchus watsoni* as a pareiasauromorph leaves Acleistorhinidae as a clade restricted to western Pangaea, now including Brazil.

Temporal openings

It appears that all acleistorhinids have temporal fenestration, although the condition is unknown in *Carbonodraco lundi* because the temporal region is unknown. Therefore, based on its phylogenetic affinities, it is expected that the Pedra de Fogo parareptile would possess a temporal fenestra as well. At first glance, the postorbital of *Karutia fortunata* does not show obvious signs that it contributed to a temporal opening. In acleistorhinids, however, the rim of the temporal fenestra is not as clearly outlined as in other parareptiles that possess this structure. The slenderness and sinuousness of the posteroventral margin of the postorbital in the Brazilian taxon is similar to the condition in other members of this clade and could represent the upper border of a temporal opening, but additional fossils are needed to confirm this feature.

The increasing recognition of lower temporal openings or ventral emarginations among several parareptile lineages (Cisneros *et al.* 2004; Tsuji 2006; Modesto *et al.* 2009; Säilä 2010; Tsuji *et al.* 2010) and evidence of temporal openings in *Mesosaurus brasiliensis* (Piñeiro *et al.* 2012; but see Modesto [2006] for a divergent perspective) has brought additional support to Cisneros *et al.*'s (2004) hypothesis that this structure is primitive for the clade. The consensus tree topology from this study supports this model, corroborating the primitive condition of temporal fenestration/emarginations and showing two instances of their loss within Parareptilia: once in Pareiasauria and once in a clade of derived nycteroleters. These two reversals may be

reduced to a single one if the placement of *Lanthanosuchus watsoni* and *Macroleter poezicus*, two genera that have weak branch support in this analysis, changes to a more basal position within Pareiasauromorpha.

Ecology and probable lifestyle

The limb bones of *Karutia fortunata* are notably long and gracile, contrasting with the robust postcranium observed in many other parareptiles, such as procolophonids, pareiasaurs and even mesosaurs. The slenderness and limb proportions of the new parareptile resemble the condition in the nycteroleter *Emeroleter levis* (Tsuji *et al.* 2012) and the eureptile genus *Araeoscelis* (Reisz *et al.* 1984). *Emeroleter levis* has been proposed to be capable of rapid movement and increased sprint speed based on locomotion studies on modern *Anolis* species (Moermond 1979; Vanhooydonck et al., 2006). In particular, the long, slender limbs, with similar epipodial/propodial lengths that result in equal moment arms for the limb segments, are thought to be key to the high mobility inferred for *Emeroleter levis* (see discussion in Tsuji *et al.* 2012). *Karutia fortunata* has a forelimb epipodial/propodial ratio (∼0.91) comparable to *Emeroleter levis* (0.89). Unfortunately, we cannot calculate the hindlimb epipodial/propodial ratio due to incompleteness of the femur, but considering the overall morphological similarity of this bone to its counterpart in *Emeroleter levis* and the great length of the fibula in *Karutia fortunata*, this ratio is expected to be comparable as well. The new parareptile is thus best interpreted as an agile, sprinting animal.

The dentition of *Karutia fortunata*, comprising sharp, conical, slightly recurved teeth, is compatible with faunivorous habits. The rapid locomotion inferred from its limb proportions may have had a role in acquiring arthropods as food items and/or avoiding predation by larger carnivorous tetrapods. The skull of *Karutia fortunata* differs from *Emeroleter levis* in lacking a large otic notch that provided support for a tympanic ear (Müller & Tsuji 2007). *Karutia fortunata* may have relied more on optical and especially chemical sensory perception, aided by the nasal capsule that was hosted by a well-developed narial shelf.

Karutia fortunata is only the third terrestrial amniote taxon (Fig. 8) discovered in the Cisuralian of Gondwana. This find complements the record of two captorhinid morphotypes found in the same formation in the Teresina area (Cisneros *et al.* 2020). In contrast to the marine vertebrates found in the southern portion of the basin, this area is dominated by bony fishes and temnospondyls which inhabited a lake or wetland system. Unlike all other tetrapods found in the study area, which were preserved in massive, silicified siltstones of lacustrine origin, the new parareptile was collected from an erosively based fine-grained sandstone indicative of a

Figure 8. Life reconstruction of *Karutia fortunata* gen. et sp. nov. Illustration by JCC.

fluvial influx of terrigenous material into the lake. Future research in these fluvio-deltaic facies may contribute to revealing a fauna of more dry-land character and provide a better picture of the terrestrial communities in the lower Permian of Gondwana.

Conclusions

Karutia fortunata is the first representative of the Acleistorhinidae in Gondwana. The new taxon is closely related to *Delorhynchus cifellii* from the Permian of Oklahoma, reinforcing similarities between the Pedra de Fogo assemblage and Cisuralian faunas from southern USA. A cladistic analysis finds the Russian parareptile

Lanthanosuchus watsoni to be related to the nycteroleterids rather than to the acleistorhinids, eliminating a ghost lineage that extended from the Kungurian to the Wordian. Acleistorhinidae is a clade restricted to western Pangaea. *Karutia fortunata* contributes to our incipient knowledge of terrestrial tetrapod diversity in the Cisuralian of Gondwana.

Acknowledgements

Supplementary material

Supplementary material for this article can be accessed here: https://doi.org/10.1080/14772019.2020.1863487.

Nomenclatural Statement

The electronic version of this article in Portable Document Format (PDF) will represent a published work according to the International Commission on Zoological Nomenclature (ICZN), and hence the new names contained in the electronic version are effectively published under that Code from the electronic edition

alone. This published work and the nomenclatural acts it contains have been registered in ZooBank, the online registration system for the ICZN. The ZooBank LSIDs (Life Science Identifiers) can be resolved and the associated information viewed through any standard web browser by appending the LSID to the prefix http://zoobank.org/. The LSID for this publication is: [urn:lsid:zoobank.org:pub:79D59764-4DA0-4C28-B4D3-C517BBF64D81]. *Karutia* gen. nov.: [urn:lsid:zoobank.org:act:B5D933DB-56F4-4DA2-8A71-116DB48E0449]. *Karutia fortunata* sp. nov.:[urn:lsid:zoobank.org:act:801AFE8F-A063-4674-8A2B-3C01F87DC422].

ORCID

Juan Carlos Cisneros (iD) http://orcid.org/0000-0001-6159-1981

Christian F. Kammerer (iD) http://orcid.org/0000-0002-0596-623X

Jörg Fröbisch (iD) http://orcid.org/0000-0002-2501-9387

Claudia Marsicano (iD) http://orcid.org/0000-0002-0121-6730

Roger M. H. Smith (iD) http://orcid.org/0000-0001-6806-1983

Martha Richter (iD) http://orcid.org/0000-0002-9806-4816

References

Bellairs, A. d'A. 1949. Observations on the snout of *Varanus*, and a comparison with that of other lizards and snakes. *Journal of Anatomy*, **83**, 116–147.

Berman, D. S., **Reisz, R. R.**, **Scott, D.**, **Henrici, A. C.**, **Sumida, S. S.** & **Martens, T.** 2000. Early Permian bipedal reptile. *Science*, **290**, 969–972.

Boonstra, L. D. 1934. Pareiasaurian studies. Part XI. The vertebral column and ribs. *Annals of the South African Museum*, **31**, 49–66.

Cabreira, S. F. & **Cisneros, J. C.** 2009. Tooth histology of the parareptile *Soturnia caliodon* from the Upper Triassic of Rio Grande do Sul, Brazil. *Acta Palaeontologica Polonica*, **54**, 743–748.

Carroll, R. L. & **Lindsay, W.** 1985. Cranial anatomy of the primitive reptile *Procolophon*. *Canadian Journal of Earth Sciences*, **22**(11), 1571–1587.

Cisneros, J. C. 2008. Taxonomic status of the reptile genus *Procolophon* from the Gondwanan Triassic. *Palaeontologia africana*, **43**, 7–17.

Cisneros, J. C. & **Schultz, C. L.** 2003. *Soturnia caliodon* n. g. n. sp., a procolophonid reptile from the Upper Triassic of Southern Brazil. *Neues Jahrbuch für Geologie und Paläontologie-Abhandlungen*, **227**, 365–380.

Cisneros, J. C., **Damiani, R.**, **Schultz, C.**, **da Rosa, A.**, **Schwanke, C.**, **Neto, L. W.** & **Aurélio, P. L.** 2004. A procolophonoid reptile with temporal fenestration from the Middle Triassic of Brazil. *Proceedings of the Royal Society of London, Series B*, **271**, 1541–1546.

Cisneros, J. C. & **Tsuji, L. A.** 2009. Nycteroleter affinities of a Permian parareptile from the South African Karoo Basin. *Acta Palaeontologica Polonica*, **54**, 165–169.

Cisneros, J. C., **Marsicano, C.**, **Angielczyk, K. D.**, **Smith, R. M.**, **Richter, M.**, **Fröbisch, J.**, **Kammerer, C. F.** & **Sadleir, R. W.** 2015. New Permian fauna from tropical Gondwana. *Nature Communications*, **6**, 8676. doi:10.1038/ncomms9676

Cisneros, J. C., **Angielczyk, K.**, **Kammerer, C. F.**, **Smith, R. M.**, **Fröbisch, J.**, **Marsicano, C. A.** & **Richter, M.** 2020. Captorhinid reptiles from the lower Permian Pedra de Fogo Formation, Piauí, Brazil: the earliest herbivorous tetrapods in Gondwana. *PeerJ*, **8**, e8719. doi:10.7717/peerj.8719

Daly, E. 1969. A new procolophonoid reptile from the Lower Permian of Oklahoma. *Journal of Paleontology*, **43**, 676–687. doi:10.2307/1302462

deBraga, M. 2003. The postcranial skeleton, phylogenetic position, and probable lifestyle of the Early Triassic reptile *Procolophon trigoniceps*. *Canadian Journal of Earth Sciences*, **40**, 527–556.

deBraga M. & **Reisz R. R.** 1996. The Early Permian reptile *Acleistorhinus pteroticus* and its phylogenetic position. *Journal of Vertebrate Paleontology*, **16**, 384–395. doi:10.1080/02724634.1996.10011328

Efremov, J. A. 1940. [New discoveries of Permian terrestrial vertebrates in Bashkiria and the Tchkalov Province.] *Comptes Rendus (Doklady)* **27**, 412–415. [In Russian.]

Efremov, J. A. 1946. [On the subclass Batrachosauria, a group of forms intermediate between amphibians and reptiles.] *Bulletin of the Academy of Science of the USSR Section of Biological Sciences*, **6**, 616–638. [In Russian.]

Ford, D. P. & **Benson, R. B. J.** 2020. The phylogeny of early amniotes and the affinities of Parareptilia and Varanopidae. *Nature Ecology & Evolution*, **4**, 57–65. doi:10.1038/s41559-019-1047-3

Goloboff, P. A., **Farris, J. S.**, **Källersjö, M.**, **Oxelmann, B.**, **Ramírez, M. J.** & **Szumik, C. A.** 2003. Improvements to resampling measures of group support. *Cladistics*, **19**, 324–332. doi:10.1016/S0748-3007(03)00060-4

Goloboff, P. A. & **Catalano, S. A.** 2016. TNT version 1.5, including a full implementation of phylogenetic morphometrics. *Cladistics*, **32**, 221–238. doi:10.1111/cla.12160

Gow, C. E. 1972. The osteology and relationships of the Millerettidae (Reptilia: Cotylosauria). *Journal of Zoology*, **167**, 219–264. doi:10.1111/j.1469-7998.1972.tb01731.x

Hamley, T., **Cisneros, J. C.** & **Damiani, R.** 2020. A procolophonid reptile from the Lower Triassic of Australia. *Zoological Journal of the Linnean Society*. zlaa056. doi:10.1093/zoolinnean/zlaa056

Haridy, Y., **MacDougall, M. J.**, **Scott, D.** & **Reisz, R. R.** 2016. Ontogenetic change in the temporal region of the early Permian parareptile *Delorhynchus cifellii* and the implications for closure of the temporal fenestra in amniotes. *PLoS ONE*, **11**, e0166819. doi:10.1371/journal.pone.0166819

Haridy, Y., **MacDougall, M. J.** & **Reisz, R. R.** 2017. The lower jaw of the Early Permian parareptile *Delorhynchus*, first evidence of multiple denticulate coronoids in a reptile. *Zoological Journal of the Linnean Society*, **184**, 791–803. doi:10.1093/zoolinnean/zlx085

Heaton, M. J. 1979. Cranial anatomy of primitive captorhinid reptiles from the Late Pennsylvanian and early Permian, Oklahoma and Texas. *Oklahoma Geological Survey Bulletin*, **127**, 1–84.

Iannuzzi, R., Neregato, R., Cisneros, J. C., Angielczyk, K. D., Rössler, R., Rohn, R., Marsicano, C., Fröbisch, J., Fairchild, T., Smith, R. M. H., Kurzawe, F., Richter, M., Langer, M. C., Tavares, T. M. V., Kammerer, C. F., Conceição, D. M. Da, Pardo, J. D. & Roesler, G. A. 2018. Re-evaluation of the Permian macrofossils from the Parnaíba Basin: biostratigraphic, palaeoenvironmental and palaeogeographical implications. Pp. 223–249 in M. C. Daly, R. A. Fuck, J. Julià, D. I. M. Macdonald & A. B. Watts (eds) *Cratonic basin formation: a case study of the Parnaíba Basin of Brazil*. Special Publications of the Geological Society, London, **472**. doi: 10.1144/SP472.14

Ivakhnenko, M. F. 1979. [Permian and Triassic procolophonids of the Russian platform.] *Akademiya Nauk SSSR*, **164**, 1–80. [In Russian.]

Ivakhnenko, M. F. 2008. [Subclass Parareptilia.] Pp. 48–85 in M. F. Ivakhnenko & E. N. Kurochkin (eds) [*Fossil vertebrates of Russia and adjacent countries. Fossil reptiles and birds. Part 1.*] GEOS, Moscow. [In Russian.]

Laurenti, J. N. 1768. *Specimen medicum, exhibens synopsin reptilium emendatam cum experimentis circa venena et antidota reptilium austriacorum*. J. T. N. de Trattnern, Vienna, 214pp. +5 plates.

Laurin, M. & Reisz, R. R. 1989. Taxonomic position and phylogenetic relationships of *Colobomycter pholeter*, a small reptile from the Lower Permian of Oklahoma. *Canadian Journal of Earth Sciences*, **26**, 544–550.

Laurin, M. & Reisz, R. 1995. A reevaluation of early amniote phylogeny. *Zoological Journal of the Linnean Society*, **113**, 165–223.

Laurin, M. & Piñeiro, G. H. 2017. A reassessment of the taxonomic position of mesosaurs, and a surprising phylogeny of early amniotes. *Frontiers in Earth Science*, **5**, 88. doi:10.3389/feart.2017.00088

Laurin, M. & Piñeiro, G. 2018. Response: Commentary: A reassessment of the taxonomic position of mesosaurs, and a surprising phylogeny of early amniotes. *Frontiers in Earth Science*, **6**, 220. doi:10.3389/feart.2018.00220

Lee, M. S. Y. 1995. Historical burden in systematics and the interrelationships of 'parareptiles'. *Biological Reviews*, **70**, 459–547.

Lee, M. S. Y. 1997. A taxonomic revision of pareiasaurian reptiles: implications for Permian terrestrial palaeoecology. *Modern Geology*, **21**, 231–298.

Lee, M. S. Y., Gow, C. E. & Kitching, J. W. 1997. Anatomy and relationships of the pareiasaur *Pareiasuchus nasicornis* from the Upper Permian of Zambia. *Palaeontology*, **40**, 307–336.

Lucas, S. G. 2002. Discussion and reply: the reptile *Macroleter*. First vertebrate evidence for correlation of Upper Permian continental strata of North America and Russia. Discussion. *Geological Society of America Bulletin*, **114**, 1174–1175.

Lucas, S. G. 2017. Permian tetrapod biochronology, correlation and evolutionary events. *Special Publications of the Geological Society, London*, **450**, 405–444.

MacDougall, M. J. & Reisz, R. 2012. A new parareptile (Parareptilia, Lanthanosuchoidea) from the Early Permian of Oklahoma. *Journal of Vertebrate Paleontology*, **32**, 1018–1026. doi:10.1080/02724634.2012.679757

MacDougall, M. J. & Reisz, R. 2014. The first record of a nyctiphruretid parareptile from the Early Permian of North America, with a discussion of parareptilian temporal fenestration. *Zoological Journal of the Linnean Society*, **172**, 616–630. doi:10.1111/zoj.12180

MacDougall, M. J., LeBlanc, A. R. & Reisz, R. R. 2014. Plicidentine in the Early Permian parareptile *Colobomycter pholeter*, and its phylogenetic and functional significance among coeval members of the clade. *PLoS ONE*, **9**, e96559. doi:10.1371/journal.pone.0096559

MacDougall, M. J., Modesto, S. P. & Reisz, R. R. 2016. A new reptile from the Richards Spur locality, Oklahoma, USA, and patterns of Early Permian parareptile diversification. *Journal of Vertebrate Paleontology*, **36**, e1179641. doi:10.1080/02724634.2016.1179641

MacDougall, M. J., Scott D., Modesto, S. P., Williams, S. A. & Reisz, R. R. 2017. New material of the reptile *Colobomycter pholeter* (Parareptilia: Lanthanosuchoidea) and the diversity of reptiles during the Early Permian (Cisuralian). *Zoological Journal of the Linnean Society*, **180**, 661–671. doi:10.1093/zoolinnean/zlw012

MacDougall, M. J., Modesto, S. P., Brocklehurst, N., Verrière, A., Reisz, R. R. & Fröbisch, J. 2018. Response: A reassessment of the taxonomic position of mesosaurs, and a surprising phylogeny of early amniotes. *Frontiers in Earth Science*, **6**, 99. doi:10.3389/feart.2018.00099

MacDougall, M. J., Brocklehurst, N. & Fröbisch, J. 2019a. Species richness and disparity of parareptiles across the end-Permian mass extinction. *Proceedings of the Royal Society B, Biological Sciences*, **286**, 20182572. doi:10.1098/rspb.2018.2572

MacDougall, M. J., Winge, A., Ponstein, J., Jansen, M., Reisz, R. R. & Fröbisch, J. 2019b. New information on the early Permian lanthanosuchoid *Feeserpeton oklahomensis* based on computed tomography. *PeerJ*, **7**, e7753. doi:10.7717/peerj.7753

Maddison, W. P. & Maddison, D. R. 2018. Mesquite: a modular system for evolutionary analysis. Version 3.51. [Updated at: http://www.mesquiteproject.org, accessed 19 July 2020].

Mann, A. McDaniel E. J., McColville, E. R. & Maddin, H. C. 2019. *Carbonodraco lundi* gen. et sp. nov., the oldest parareptile, from Linton, Ohio, and new insights into the early radiation of reptiles. *Royal Society Open Science*, **6**, 191191. doi:10.1098/rsos.191191

Meckert, D. 1995. *The procolophonid* Barasaurus *and the phylogeny of early amniotes*. Unpublished PhD dissertation, McGill University, Montréal, 149 pp.

Modesto, S. P. 1998. New information on the skull of the Early Permian reptile *Captorhinus aguti*. *PaleoBios*, **18**, 21–35.

Modesto, S. P. 1999. *Colobomycter pholeter* from the Lower Permian of Oklahoma: a parareptile, not a protorothyridid. *Journal of Vertebrate Paleontology*, **19**, 466–472.

Modesto, S. P. 2006. The cranial skeleton of the Early Permian aquatic reptile *Mesosaurus tenuidens*: implications for relationships and palaeobiology. *Zoological Journal of the Linnean Society*, **146**, 345–368.

Modesto, S. P. 2010. The postcranial skeleton of the aquatic parareptile *Mesosaurus tenuidens* from the Gondwanan

Permian. *Journal of Vertebrate Paleontology*, **30**, 1378–1395. doi:10.1080/02724634.2010.501443

Modesto, S. P. & Reisz, R. R. 2008. New material of *Colobomycter pholeter*, a small parareptile from the Lower Permian of Oklahoma. *Journal of Vertebrate Paleontology*, **28**, 677–684.

Modesto, S. P., Scott, D. M. & Reisz, R. R. 2009. A new parareptile with temporal fenestration from the Middle Permian of South Africa. *Canadian Journal of Earth Sciences*, **46**, 9–20.

Modesto, S. P., Scott, D. M., MacDougall, M. J., Sues, H.-D., Evans, D. C. & Reisz, R. R. 2015. The oldest parareptile and the early diversification of reptiles. *Proceedings of the Royal Society B, Biological Sciences*, **282**, 20141912. doi:10.1098/rspb.2014.1912

Moermond, T. C. 1979. Habitat constraints on the behavior, morphology, and community structure of *Anolis* lizards. *Ecology*, **60**, 152–164.

Müller, J. & Tsuji, L. A. 2007. Impedance-matching hearing in Paleozoic reptiles: evidence of advanced sensory perception at an early stage of amniote evolution. *PLoS ONE*, **2**, e889. doi:10.1371/journal.pone.0000889

Olson, E. C. 1947. The Family Diadectidae and its bearing on the classification of reptiles. *Fieldiana: Geology*, **11**(1), 1–53.

Piñeiro, G., Ramos, A., Goso, C., Scarabino, F. & Laurin, M. 2012. Unusual environmental conditions preserve a Permian mesosaur-bearing Konservat-Lagerstätte from Uruguay. *Acta Palaeontologica Polonica*, **57**, 299–318.

Reisz, R. R. 2006. Origin of dental occlusion in tetrapods: signal for terrestrial vertebrate evolution? *Journal of Experimental Zoology Part B: Molecular and Developmental Evolution*, **306**(3), 261–277.

Reisz, R. R., Berman, D. S. & Scott, D. 1984. The anatomy and relationships of the Lower Permian reptile *Araeoscelis*. *Journal of Vertebrate Paleontology*, **4**, 57–67.

Reisz, R. R. & Sues, H.-D. 2000. Herbivory in late Paleozoic and Triassic terrestrial vertebrates. Pp. 9–41 in H.-D. Sues (ed.) *Evolution of herbivory in terrestrial vertebrates: perspectives from the fossil record*. Cambridge University Press, Cambridge.

Reisz, R. R. & Laurin, M. 2001. The reptile *Macroleter*: first vertebrate evidence for correlation of Upper Permian continental strata of North America and Russia. *Geological Society of America Bulletin*, **113**, 1229–1233.

Reisz, R. R. & Laurin, M. 2002. Discussion and reply: The reptile *Macroleter*: first vertebrate evidence for correlation of Upper Permian continental strata of North America and Russia – Reply. *Geological Society of America Bulletin*, **114**, 1176–1177. doi:10.1130/0016-7606(2002)114 < 1176:R > 2.0.CO;2

Reisz, R. R. & Scott, D. 2002. *Owenetta kitchingorum*, sp. nov., a small parareptile (Procolophonia: Owenettidae) from the Lower Triassic of South Africa. *Journal of Vertebrate Paleontology*, **22**, 244–256.

Reisz, R. R., Müller, J., Tsuji, L. & Scott, D. 2007. The cranial osteology of *Belebey vegrandis* (Parareptilia: Bolosauridae), from the Middle Permian of Russia, and its bearing on reptilian evolution. *Zoological Journal of the Linnean Society*, **151**, 191–214.

Reisz, R. R., MacDougall, M. J. & Modesto, S. P. 2014. A new species of the parareptile genus *Delorhynchus*, based on articulated skeletal remains from Richards Spur, Lower Permian of Oklahoma. *Journal of Vertebrate Paleontology*, **34**, 1033–1043.

Ruta, M., Cisneros, J. C., Liebrecht, T., Tsuji, L. A. & Müller, J. 2011. Amniotes through major biological crises: faunal turnover among parareptiles and the end-Permian mass extinction. *Palaeontology*, **54**, 1117–1137. doi:10.1111/j.1475-4983.2011.01051.x

Säilä, L. K. 2008. The osteology and affinities of *Anomoiodon liliensterni*, a procolophonid reptile from the Lower Triassic Bundsandstein of Germany. *Journal of Vertebrate Paleontology*, **28**, 1199–1205.

Säilä, L. K. 2010. The phylogenetic position of *Nyctiphruretus acudens*, a parareptile from the Permian of Russia. *Journal of Iberian Geology*, **36**, 123–143.

Snyder, A. J., LeBlanc, A. R. H., Jun, C., Bevitt, J. J. & Reisz, R. R. 2020. Thecodont tooth attachment and replacement in bolosaurid parareptiles. *PeerJ*, **8**, e9168. doi:10.7717/peerj.9168

Tsuji, L. A. 2006. Cranial anatomy and phylogenetic affinities of the Permian parareptile *Macroleter poezicus*. *Journal of Vertebrate Paleontology*, **26**, 849–865.

Tsuji, L. A. & Müller, J. 2009. Assembling the history of the Parareptilia: phylogeny, diversification, and a new definition of the clade. *Fossil Record*, **12**, 71–81. doi:10.1002/mmng.200800011

Tsuji, L. A., Müller, J. & Reisz, R. R. 2010. *Microleter mckinzieorum* gen. et sp. nov. from the Lower Permian of Oklahoma: the basalmost parareptile from Laurasia. *Journal of Systematic Palaeontology*, **8**, 245–255.

Tsuji, L. A., Müller, J. & Reisz, R. R. 2012. Anatomy of *Emeroleter levis* and the phylogeny of the nycteroleter parareptiles. *Journal of Vertebrate Paleontology*, **32**, 45–67. doi:10.1080/02724634.2012.626004

Vanhooydonck, B., Herrel, A., Damme, R. V. & Irschick, D. J. 2006. The quick and the fast: the evolution of acceleration capacity in *Anolis* lizards. *Evolution*, **60**, 2137–2147.

Vaughn, P. P. 1958. On a new pelycosaur from the Lower Permian of Oklahoma, and on the origin of the family Caseidae. *Journal of Paleontology*, **32**, 981–991.

Verrière, A., Brocklehurst, N. & Fröbisch, J. 2016. Assessing the completeness of the fossil record: comparison of different methods applied to parareptilian tetrapods (Vertebrata: Sauropsida). *Paleobiology*, **42**, 680–695. doi:10.1017/pab.2016.26

Watson, D. M. S. 1954. On *Bolosaurus* and the origin and classification of reptiles. *Bulletin of the Museum of Comparative Zoology*, **111**, 297–449.

Associate Editor: Jennifer Olori